DOI：10.16410/j.issn1000-8365.2025.5117

数据驱动结晶器液位波动与卷渣缺陷相关性研究

陆志豪[1,2]，赵晨光[3]，马永东[4]，陈　宇[3]，尚世震[3]，李博洋[1,2]，贾吉祥[1,2]
(1. 海洋装备金属材料及其应用全国重点实验室，辽宁 鞍山 114009；2. 鞍钢集团钢铁研究院，辽宁 鞍山 114009；3. 鞍钢股份有限公司 炼钢总厂，辽宁 鞍山 114009；4. 鞍钢集团朝阳钢铁有限公司，辽宁 朝阳 122000)

摘　要：在现代 IF 钢连铸工艺中，结晶器液位的稳定性对铸坯质量具有重要影响。液位波动可能导致保护渣卷入钢液形成夹杂缺陷，降低钢材的纯净度和最终性能。传统连铸过程监测主要依赖物理实验和有限元模拟，而随着工业数据采集能力的提升，数据驱动分析方法在工艺优化中展现出巨大潜力。针对 IF 钢连铸过程，通过采集工业生产中的液位波动数据、卷渣夹杂检测信息及相关工艺参数，运用统计分析、时序分析和机器学习方法，探索了结晶器液位波动特征及其对保护渣卷入的影响机理，提出了优化控制策略。研究结果表明，液位波动的多个特征参数与卷渣夹杂缺陷之间存在显著相关性，通过优化控制策略可有效降低夹杂物发生的概率。

关键词：IF 钢；连铸工艺；结晶器液位波动；卷渣缺陷；数据驱动分析

中图分类号：TG2; TF777.1　　文献标识码：A　　文章编号：1000-8365(2025)10-0964-09

Data-driven Correlation Analysis of Mold Level Fluctuation and Slag Entrapment Defects

LU Zhihao[1,2], ZHAO Chenguang[3], MA Yongdong[4], CHEN Yu[3], SHANG Shizhen[3], LI Boyang[1,2], JIA Jixiang[1,2]
(1. State Key Laboratory of Metal Material for Marine Equipment and Application, Anshan 114009, China; 2. Ansteel Iron & Steel Research Institutes, Anshan 114009, China; 3. General Steelmaking Plant of Angang Steel Co., Ltd., Anshan 114009, China; 4. Chaoyang Iron & Steel Co., Ltd. of Ansteel Group Corporation, Chaoyang 122000, China)

Abstract: In modern interstitial-free (IF) steel continuous casting processes, the stability of the mold level plays a critical role in determining slab quality. Excessive fluctuations may cause slag entrapment into molten steel, resulting in inclusion defects that degrade the purity and final mechanical properties of the steel. While traditional process monitoring primarily depends on physical experiments and finite element simulations, the advancement of industrial data acquisition technologies has enabled data-driven approaches to demonstrate significant potential for process optimization. Industrial IF steel casting operations involving the collection of mold level fluctuation data, slag entrapment records, and associated process parameters were investigated. Through integrated statistical analysis, time series characterization and machine learning techniques, the intrinsic relationship between mold-level fluctuation patterns and slag entrapment mechanisms was systematically explored, and corresponding control strategies were proposed. The results demonstrate significant correlations between the characteristic parameters of level fluctuations and slag entrapment defects. The implementation of optimized control strategies effectively reduces the probability of inclusion formation.

Key words: interstitial-free steel; continuous casting process; mold level fluctuation; slag entrapment defect; data-driven analysis

在现代 IF(interstitial-free)钢连铸生产过程中，结晶器是影响铸坯质量的关键工序之一[1]。结晶器内钢液液位的稳定性对于控制夹杂物、保证钢材高纯净度以及提升产品表面质量至关重要[2-4]。作为钢液初步凝固的场所，结晶器液位波动可能引发一系列质量问题，其中尤以保护渣卷入(entrapped slag)导致的非金属夹杂缺陷最为突出[5-6]。这类夹杂不仅影响钢材的均匀性，还可能在后续轧制和深冲加工过

收稿日期：2025-06-20
基金项目：辽宁省技术攻关计划(2024JH2/102600056)
作者简介：陆志豪，1992 年生，博士，副研究员．主要从事绿色化智慧化炼钢技术开发方面的工作．Email: lzh_ansteel@163.com
引用格式：陆志豪，赵晨光，马永东，陈宇，尚世震，李博洋，贾吉祥．数据驱动结晶器液位波动与卷渣缺陷相关性研究[J]. 铸造技术，2025, 46(10): 964-972.
LU Z H, ZHAO C G, MA Y D, CHEN Y, SHANG S Z, LI B Y, JIA J X. Data-driven correlation analysis of mold level fluctuation and slag entrapment defects[J]. Foundry Technology, 2025, 46(10): 964-972.

程中引发裂纹、表面缺陷等，降低材料力学性能，缩短其在汽车、高端电工钢等领域的服役寿命[7]。因此，深入研究结晶器液位波动与 IF 钢夹杂缺陷之间的关系对于优化连铸工艺、提高钢材质量、降低夹杂含量具有重要的理论意义和工程价值。近年来，随着在线测量技术、智能传感器和数据分析方法的快速发展，使得数据驱动方法在钢铁生产各环节均有较好的应用案例[8-15]，随着连铸过程的数据采集与分析能力显著提升，卷渣问题的数智化研究手段也不再仅依靠计算机数值模拟[16-22]，利用数据驱动的方法研究液位波动与夹杂物形成的关系已成为可能[23-25]。驱动分析能够从大量生产数据中提取影响夹杂物的关键变量，建立量化的关系模型，为连铸工艺的智能优化提供理论依据。通过深入分析结晶器液位的波动特征，并结合夹杂物检测数据，采用时序分析、机器学习建模和相关性分析等方法，可以研究液位波动对夹杂缺陷的影响机制，并提出相应的优化控制策略，以减少液位波动对 IF 钢纯净度的不利影响。为此，本研究构建了数据驱动的液位波动-夹杂缺陷相关性分析模型，为高品质 IF 钢连铸工艺的优化提供指导。

1 样品及数据采集

1.1 IF 钢卷渣缺陷分析

在 IF 钢连铸过程中，结晶器液位波动是影响钢坯质量的重要因素之一。过大的液位扰动可能导致保护渣卷入钢液，形成非金属夹杂物，进而降低钢材的纯净度和性能。通过对某钢厂生产的 IF 钢样品进行扫描电子显微镜(SEM)和能谱分析(EDS)，如图 1 所示，发现夹杂物中含有 Na 和 F 元素。这是典型的保护渣成分，也是卷渣类夹杂的标志物[5]，现场生产经验指出，卷渣现象与结晶器内液位波动有关。引起液位波动的原因复杂，可能是水口结瘤、氩气流、拉速不稳定、结晶器电磁搅拌(electromagnetic stirring, EMS)等因素扰动了结晶器内的钢液流场[26]。当液位波动幅度超过特定阈值(该阈值与设备情况，钢种情况高度相关)时，弯月面处渣-钢界面被破坏，保护渣进入钢液并被初生坯壳捕获而无法上浮，最终在凝固过程中形成夹杂[27]。基于此，本研究将结合结晶器液位的在线监测数据，利用数据驱动方法分析液位波动与保护渣卷入之间的关联，并通过液位波动特征参数(如波动幅度、频率等)来量化卷渣发生的概

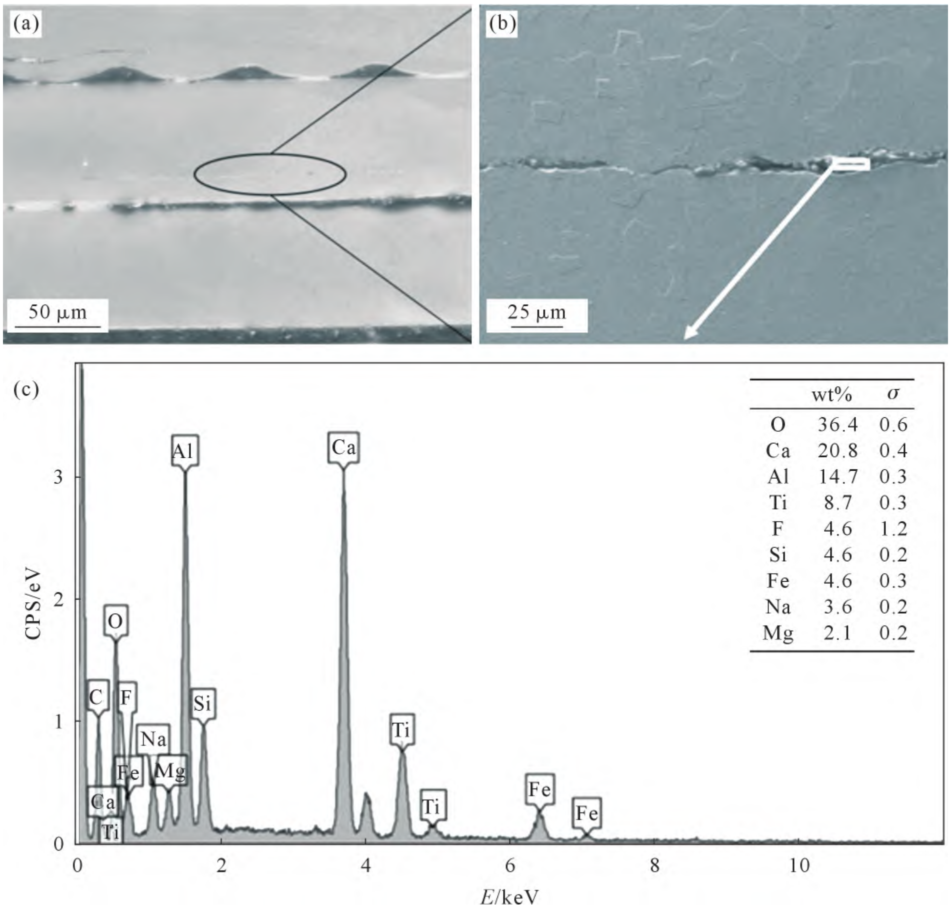

	wt%	σ
O	36.4	0.6
Ca	20.8	0.4
Al	14.7	0.3
Ti	8.7	0.3
F	4.6	1.2
Si	4.6	0.2
Fe	4.6	0.3
Na	3.6	0.2
Mg	2.1	0.2

图 1 某厂生产的 IF 钢板材缺陷 SEM 分析结果：(a) 缺陷宏观图；(b) 缺陷微观图及 EDS 检测位置；(c) EDS 检测结果

Fig.1 SEM analysis results of defects in IF steel sheets produced by a certain plant: (a) macrograph of the defect; (b) micrograph of the defect and EDS detection location; (c) EDS spectrum results

率，进一步探讨优化结晶器液位控制策略的方法，以降低液位波动导致的卷渣风险、提高铸坯纯净度。

1.2 IF 钢生产数据采集

为了研究结晶器液位波动与 IF 钢卷渣缺陷之间的关系，采集了某钢厂连铸生产过程中 81 组数据样本，其中 33 组存在卷渣缺陷，另外 48 组未出现缺陷。所有数据均取自铸机稳定浇铸阶段，不包含浇注初段和结束段，以排除浇注始末阶段液位扰动的影响，从而反映整体工况。同时，所选取生产数据中各组别拉速参数保持一致，排除拉速变化对液位波动造成干扰的情况，使所采集的液位数据能够更直接地反映卷渣缺陷的影响因素。尽管数据样本数量(81 组)较少，但由于所有样本均来源于工艺稳定阶段，具有较高的代表性和数据质量，这在工业现场的研究中是较为常见的情况[28]。此外，通过严格控制拉速和其他关键参数，有效降低了外部干扰，从而使得有限样本数据依然能为液位波动与卷渣缺陷之间的关系提供可靠依据。利用交叉验证、bootstrapping 以及稳健统计检验方法(如 t 检验和 Mann-Whitney U 检验)进一步增强了模型的鲁棒性和结果的可信度[29]。

1.3 IF 特征提取与处理

在连铸过程中，结晶器内钢液液位的波动是引发卷渣缺陷的重要因素之一。剧烈的液位波动可能导致保护渣卷入钢液，形成夹杂缺陷。因此，准确提取和分析液位波动特征对于预测和控制卷渣风险具有重要意义。液位波动的产生受到拉速波动、气泡上浮、流场扰动等因素的影响，其波动幅度、频率以及突变特征均可能与卷渣缺陷相关。鉴于此，本研究从物理机制分析和数据驱动方法相结合的角度出发，在基础统计特征、动态时序特征和频域特征 3 个方面共提取了 27 项特征参数，以全面表征液位波动行为，建立多维度的液位波动分析框架[30-35]。各类特征指标说明见表 1~3。

2 实验结果

2.1 特征相关性分析及优化

为评估不同液位波动特征与卷渣缺陷之间的相关性，采用 Pearson 和 Spearman 相关系数分析，并结合随机森林模型的特征重要性，对提取的特征进行筛选以找出对卷渣预测贡献最大的特征。原始特征集的 Pearson 相关性热力图如图 2a 所示，可以看

表1 基础统计特征
Tab.1 Basic statistical characteristics

No.	Characteristic	Definition	Calculation formula	
1	$\bar{x}$/m	Mean value: Measures the average level of the sequence over the entire sampling period	$\bar{x}=\frac{1}{N}\sum_{i=1}^{N}X_i$	(1)
2	σ/m	Standard deviation: Describes the degree of data dispersion around the mean	$\sigma=\sqrt{\frac{1}{N}\Sigma_{i=1}^{N}(x_i-\bar{x})^2}$	(2)
3	min/m	Minimum value: The smallest value in the sequence over the entire time period	$\min(x_i), i=1, \cdots, N$	(3)
4	max/m	Maximum value: The largest value in the sequence over the entire time period	$\max(x_i), i=1, \cdots, N$	(4)
5	Range/m	Fluctuation range: The difference between the maximum and minimum values	$\mathrm{Range}=\max(x_i)-\min(x_i)$	(5)
6	median/m	Median: The value at the middle position after sorting the data by magnitude	$\mathrm{median}(x_1, x_2, \cdots, x_N)$	(6)
7	cv	Coefficient of variation: Ratio of standard deviation to the mean, measuring relative fluctuation (dimensionless)	$cv=\frac{\sigma}{\bar{x}}$	(7)
8	RMS/m	Root mean square: Reflects the overall energy or amplitude level of the data	$\mathrm{RMS}=\sqrt{\frac{1}{N}\Sigma_{i=1}^{N}x_i^2}$	(8)
9	MAD/m	Mean adjacent difference: Average of differences between adjacent sampling points, measuring the average rate of change	$\mathrm{MAD}=\frac{1}{N-1}\Sigma_{i=2}^{N}(x_i-x_{i-1})$	(9)
10	S	Skewness: Indicator of distribution symmetry; a positive value indicates right skewness, while a negative value indicates left skewness (dimensionless)	$S=\frac{1}{N}\Sigma_{i=1}^{N}\left(\frac{x_i-\bar{x}}{\sigma}\right)^3$	(10)
11	K	Kurtosis: Indicates the degree of peakedness or flatness of the distribution; a larger value implies a sharper peak or heavier tails (dimensionless)	$K=\frac{1}{N}\Sigma_{i=1}^{N}\left(\frac{x_i-\bar{x}}{\sigma}\right)^4-3$	(11)

表2 动态与时间序列特征

Tab.2 Dynamic and time–series characteristics

No.	Characteristic	Definition	Calculation formula	
12	$\Delta x_i/(\mathrm{m\cdot s^{-1}})$	First-order derivative mean: Measures the overall upward or downward trend of liquid level/pull speed	$\Delta x_i=x_i-x_{i-1}, \mathrm{mean}(\Delta x)=\frac{1}{N-1}\Sigma_{i=2}^{N}\Delta x_i$	(12)
13	$\mathrm{Std}(\Delta x)/(\mathrm{m\cdot s^{-1}})$	Standard deviation of first-order derivative: Measures the fluctuation amplitude of the derivative (speed variation)	$\mathrm{Std}(\Delta x)=\sqrt{\frac{1}{N}\Sigma(\Delta x_i-\overline{\Delta x})^2}$	(13)
14	$\mathrm{Range}(\Delta x)/(\mathrm{m\cdot s^{-1}})$	Range of first-order derivative: The difference between the maximum and minimum values of the first-order derivative	$\mathrm{Range}(\Delta x)=\max(\Delta x_i)-\min(\Delta x_i)$	(14)
15	$\Delta^2 x_i/(\mathrm{m\cdot s^{-2}})$	Second-order derivative mean: The average of second-order derivatives, representing overall acceleration	$\Delta^2 x_i=\Delta x_i-\Delta x_{i-1},\ \mathrm{mean}(\Delta^2 x_i)=\frac{1}{N-2}\Sigma_{i=3}^{N}\Delta^2 x_i$	(15)
16	$\mathrm{Std}(\Delta^2 x)/(\mathrm{m\cdot s^{-2}})$	Standard deviation of second-order derivative: The fluctuation degree of acceleration over time	$\mathrm{Std}(\Delta^2 x)=\sqrt{\frac{1}{N-2}\Sigma(\mathrm{d}x_i\cdot\overline{\Delta^2 x})^2}$	(16)
17	$\mathrm{Range}(\Delta^2 x)/(\mathrm{m\cdot s^{-2}})$	Range of second-order derivative: The difference between the maximum and minimum values of the second-order derivative	$\mathrm{Range}(\Delta^2 x)=\max(\Delta^2 x_i)-\min(\Delta^2 x_i)$	(17)
18	$\mathrm{Range}(\overline{x_{3s}})/\mathrm{m}$	Variation range of 3-second window mean: Calculate the mean within a 3-second sliding window, then statistically find the difference between the maximum and minimum of these means	$\mathrm{Range}(\overline{x_{3s}})=\max(\overline{x_{3s}})-\min(\overline{x_{3s}})$	(18)
19	$\mathrm{Range}(\sigma_{3s})/\mathrm{m}$	Variation range of 3-second window standard deviation: Calculate the standard deviation within a 3-second sliding window, then statistically find the difference between the maximum and minimum of these standard deviations	$\mathrm{Range}(\sigma_{3s})=\max(\sigma_{3s})-\min(\sigma_{3s})$	(19)
20	$t_{\mathrm{recovery}}/\mathrm{s}$	Liquid level recovery time: The time needed for the liquid level to return to the set mean after exceeding the steady-state threshold	$t_{\mathrm{recovery}}=\min\{t{:}x(t)$ recovers to the steady-state interval$\}$	(20)
21	NAF/times	Number of abnormal fluctuations: Count the times when the instantaneous change (or derivative) exceeds a threshold (e.g., 3σ).	$\mathrm{NAF}=\Sigma_{i=2}^{N}(\lvert x_i-x_{i-1}\rvert>k\sigma_\Delta)$	(21)

表3 频域特征

Tab.3 Frequency–response characteristics

No.	Characteristic	Definition	Calculation formula	
22	Overshoot/m	Liquid level overshoot magnitude: The maximum deviation of the liquid level from the steady-state value or mean	$\mathrm{Overshoot}=\max(x_i-\bar{x})$	(22)
23	NO/times	Liquid level overshoot times: Count of times the liquid level exceeds the steady-state interval (e.g., ±δ from the mean)	$\mathrm{NO}=\Sigma_{i=2}^{N}(\lvert x_i-\bar{x}\rvert>\delta)$	(23)
24	Normalized Std	Liquid level fluctuation magnitude (normalized standard deviation): $\sigma/\bar{x}$ or similar to the coefficient of variation (but normalized for specific intervals, dimensionless)	Normalized Std=mean(x)/Std(x)	(24)
25	$f_{\mathrm{dom}}/\mathrm{Hz}$	Dominant frequency: The frequency component with the maximum energy, identified via FFT or Welch's method	$f_{\mathrm{dom}}=\arg f_{\max}[\mathrm{PSD}(f)]$	(25)
26	$T_{\mathrm{dom}}/\mathrm{s}$	Fluctuation period: Reciprocal of the dominant frequency, representing the periodic length of the main oscillations (liquid level or pull speed)	$T_{\mathrm{dom}}=1/f_{\mathrm{dom}}$	(26)
27	Fluctuation energy, E/m^2	Fluctuation energy: Integrate the power spectral density (PSD) over the dominant frequency band to quantify fluctuation intensity	$E=\Sigma_{f\in\mathrm{band}}\mathrm{PSD}(f)\Delta f$	(27)

到某些特征在 $|r|>0.8$ 区域内高度聚集，表明特征之间存在显著的多重共线性[36]。本研究在特征选择中采取了以模型驱动为导向的策略：对于相关性较高的冗余特征，保留随机森林重要性更高者，而非简单选择与目标变量相关系数更高者。优化后的特征相关性热力图如图 2b 所示。经过筛选最终保留特征 13 项，包括：液位超调幅度、标准差、二阶导数均值、异常波动次数、中位数、平均相邻差、液位恢复时间、

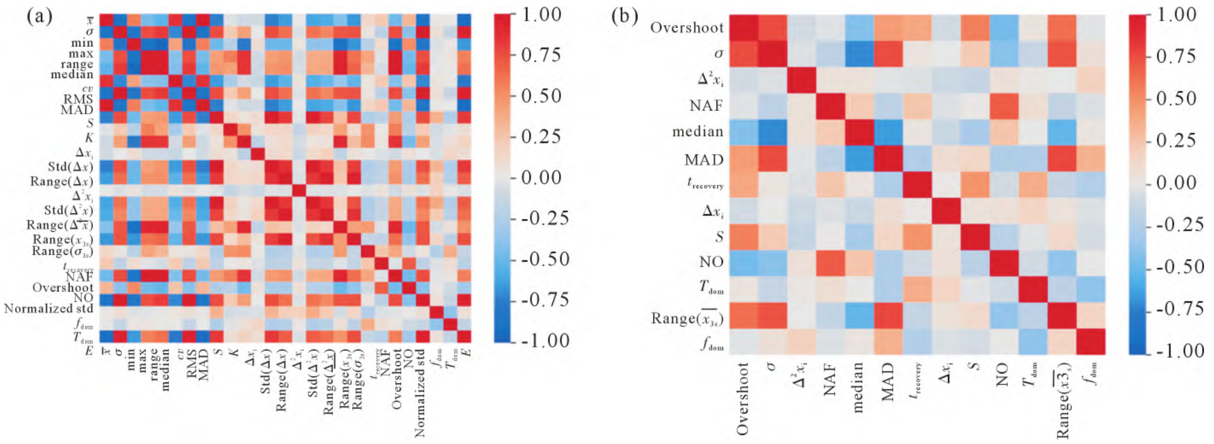

图 2 特征集 Pearson 相关性热力图:(a) 原始特征集;(b) 优化特征集
Fig.2 Pearson correlation heatmaps of feature sets: (a) original feature set; (b) optimized feature set

一阶导数均值、偏度、液位超调次数、波动周期、3 s 窗口标准差变化范围和主频率。综上,本研究建立了一套液位波动特征提取与分析的框架,可用于连铸工况的监测和卷渣缺陷的早期预警。未来将进一步结合深度学习技术,优化特征融合策略,提高预测模型的准确性和泛化能力。

2.2 特征重要性分析及优化

完成冗余特征筛选后,进一步采用随机森林模型和差异性检验方法对保留特征进行定量评价[37-38]。在随机森林模型中,比较了原始特征集和优化后特征集的特征重要性,如图 3 所示。结果表明,特征数量减少后,随机森林的预测性能并未下降,模型结构更简洁且易于解释。模型分析发现,表征液位波动幅度和变化速率的特征(如液位波动幅度、液位变化率、最大上升速率)以及频率特征(如液位主频率)对卷渣缺陷的预测贡献较高。

具体而言,针对优化后的特征集,随机森林计算的特征重要性显示:“标准差”(重要性 0.115 1)和“液位超调幅度”(0.113 1)在模型判别中贡献最大,“3 s 窗口标准差变化范围”(0.107 2)和“平均相邻差”(0.088 3)次之,而“液位超调次数”(0.082 6)和“中位数”(0.072 9)等特征也具有较高的重要性。同时,本文对卷渣缺陷发生组与未发生组的样本分别进行了 t检验和 Mann-Whitney U 检验,并以两种检验中较小的 p 值作为特征差异显著性的评价指标。图 4 展示了主要特征在两组样本中的值分布差异箱线图,其中箱体的上下缘分别代表第 25%和第 75%分位数,中线表示中位数,离群值以独立符号标示。

统计检验结果表明:“标准差”特征 p=0.003 6 和“液位超调幅度”特征 p=0.008 3,“3 秒窗口标准差变化范围”特征 p=0.009 1,“平均相邻差”特征 p=0.038 3,在统计层面同样表现出显著差异,与随机森林排名相互印证,而“液位超调次数”特征 p=0.099 2,介于 0.05 与 0.1 之间,体现出边界性显著。整体而言,那些在模型贡献度和统计差异性方面均表现突出的特征多与钢液液位波动的强度或持续性密切相关。这说明当诸如“标准差”或“液位超调幅度”等指标持续升高时,结晶器内渣-钢界面更易被强烈冲击而破碎,保护渣卷入钢液的风险也显著增加。

3 讨论

综合随机森林特征重要性与统计检验结果可知,“标准差”“液位超调幅度”“3 s 窗口标准差变化范围”和“平均相邻差”等特征在区分卷渣缺陷方面

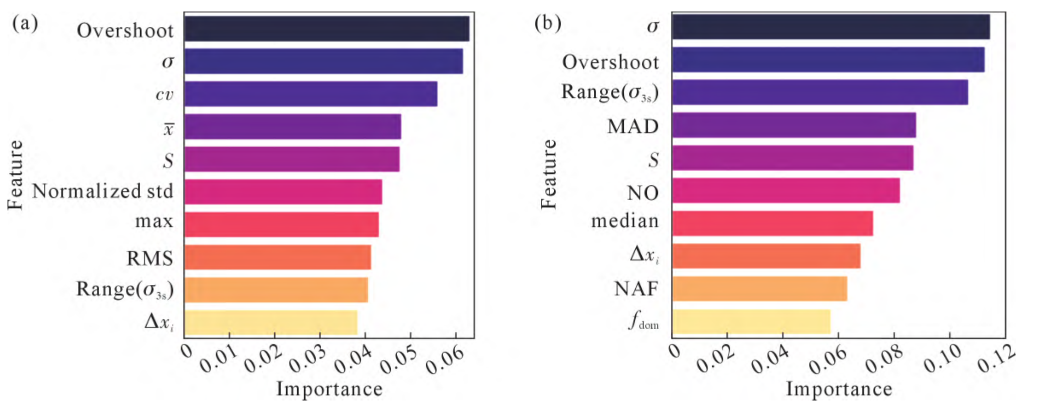

图 3 随机森林模型特征重要性分析:(a) 原始特征集;(b) 优化特征集
Fig.3 Feature importance analysis via the random forest model: (a) original feature set; (b) optimized feature set

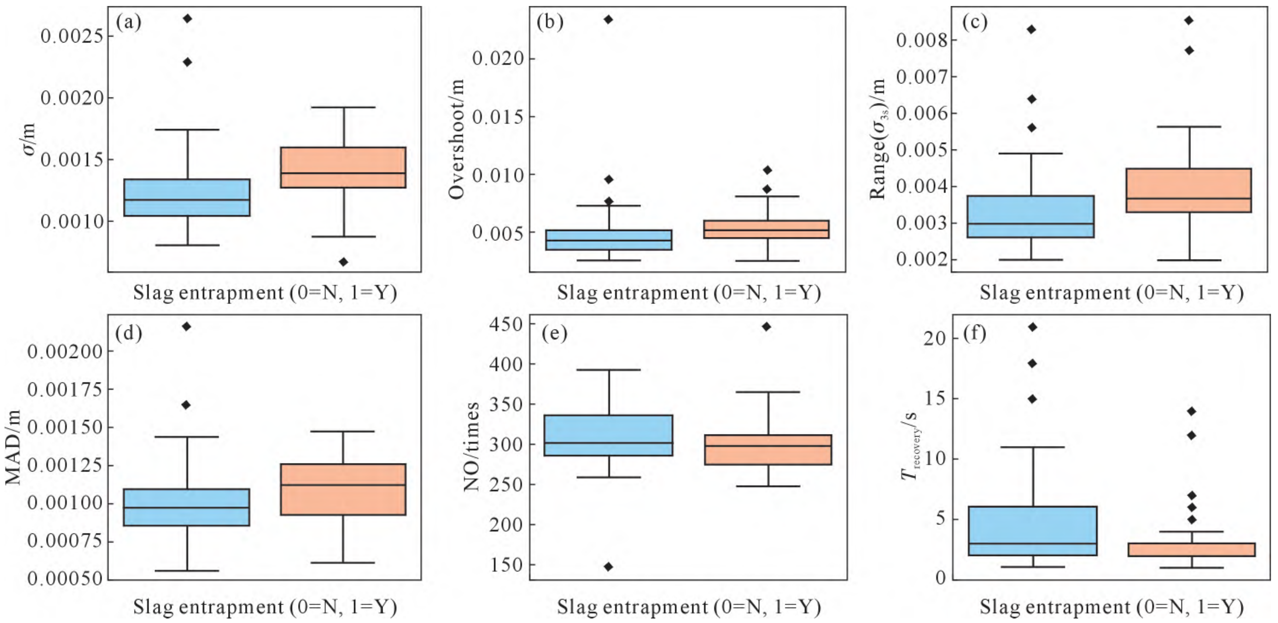

图 4　t 检验与 Mann-Whitney U 检验的特征显著性分析:(a) 标准差;(b) 液位超调幅度;(c) 3 秒窗口标准差变化范围;(d) 平均相邻差;(e) 液位超调次数;(f) 液位恢复时间

Fig.4　Statistical significance testing of features via the t test and Mann-Whitney U test: (a) standard deviation; (b) liquid level overshoot magnitude; (c) variation range of standard deviation within a 3-second window; (d) mean adjacent difference; (e) liquid level overshoot times; (f) liquid level recovery time, $t_{recovery}$

表现最为突出。其中,“标准差”在随机森林中排名首位且 p 值最小,表明其对卷渣缺陷的预测和机理解释具有极强的区分能力;“液位超调幅度”同样在模型贡献度和统计显著性上表现出色,提示当液位出现较大超调时保护渣层更容易被冲击破坏;“3 s 窗口标准差变化范围”反映短时间内液位波动的剧烈程度,对瞬时扰动引发的卷渣现象有明显的指示作用;而“平均相邻差”的模型重要性虽略低于前 3 项,但其 p 值依然达到显著水平,说明该特征对卷渣缺陷识别具有较好的补充价值。这些特征从波动幅度、短时极值和局部扰动速率等多个角度量化了钢液对渣–钢界面的冲击强度,与卷渣缺陷的形成机理紧密吻合。在后续研究和实际生产中,应重点监控这些特征参数并设定合理的报警阈值,实现对结晶器液位波动和卷渣风险更加精确的预警和有效控制。

在对 27 项特征进行 Pearson & Spearman 相关性分析并结合随机森林排名后,共保留 13 项特征以进一步评估。随后又根据差异性分析的 p 值与随机森林重要性分值,对这 13 项特征进行了二次筛选,最终选出“标准差”“液位超调幅度”“3 秒窗口标准差变化范围”与“平均相邻差”4 个关键特征。本节围绕这 4 个特征展开 F_1 分数[39]阈值分析,获得兼顾精确率与召回率的最优预警线,并在工业现场中减少漏报带来的高额损失。

基于以上识别的关键液位波动特征,进一步分析了其用于卷渣缺陷检测的最佳阈值设定。图 5 展示了对“标准差”“液位超调幅度”“3 s 窗口标准差变化范围”和“平均相邻差”4 项特征进行的 F_1 分数最优阈值分析。定量结果表明,标准差在阈值 0.001 34 m 处可获得精确率 0.657、召回率 0.697(F_1= 0.676);液位超调幅度在阈值 0.004 75 m 时精确率和召回率分别达到 0.615 和 0.727(F_1=0.667)。相比之下,3 s 窗口标准差变化范围取判定阈值0.003 02 m 时召回率可提高至 0.879,但精确率仅为 0.558(F_1= 0.682);平均相邻差阈值 0.000 84 m 时召回率高达 0.909, 但精确率偏低(仅 0.455,F_1=0.606)。可以看到,“标准差”和“液位超调幅度”在保证较高召回率的同时也保持了相对平衡的精确率;而“3 s 窗口标准差变化范围”和“平均相邻差”则更侧重于捕捉剧烈或短时的局部液位波动,显著提升了对卷渣缺陷发生的敏感度(高召回率),但相应降低了检测的精确率。由此可见,各特征在卷渣缺陷识别中各有侧重,应根据具体生产需求调节其判定阈值,或者将多个特征指标结合形成联合判别策略,以同时兼顾减少漏检(提升召回率)和降低误报(提高精确率)的目标。

4　结论

(1)结合 Pearson 相关性分析与随机森林特征重要性评估,结晶器液位波动与铸坯卷渣缺陷具有相关性,液位波动的“标准差”“液位超调幅度”“3 秒窗口标准差变化范围”“平均相邻差”等特征在统计检

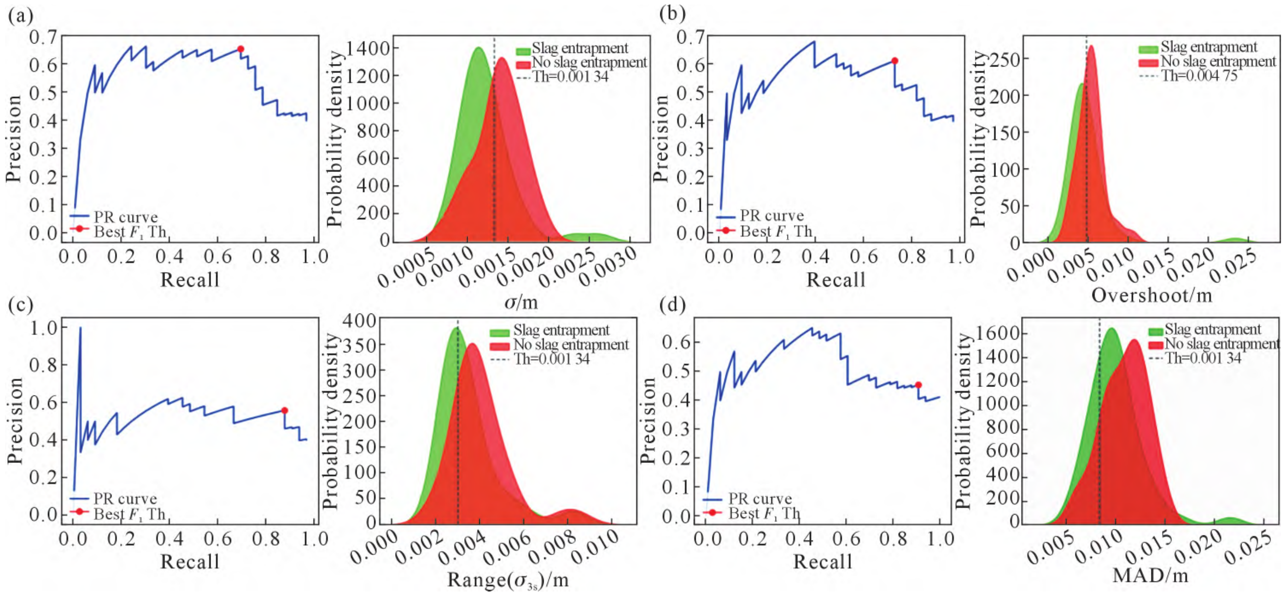

图 5 特征值最佳阈值分析:(a) 标准差; (b) 液位超调幅度;(c) 3 s 窗口标准差变化范围;(d) 平均相邻差

Fig.5 Optimal threshold determination for feature values: (a) standard deviation; (b) liquid level overshoot magnitude; (c) variation range of standard deviation within a 3-second window; (d) mean adjacent difference

验与模型贡献度方面均表现突出。

(2)标准差在阈值 0.001 34 m 时,对发生卷渣缺陷判断的精确率为 0.657、召回率≈0.697(F_1=0.676);液位超调幅度阈值 0.004 75 m 时,对发生卷渣缺陷判断的精确率为 0.615、召回率≈0.727(F_1=0.667);3 秒窗口标准差变化范围阈值 0.003 02 m 时,对发生卷渣缺陷判断的召回率可达 0.879, 精确率降至 0.558(F_1=0.682);平均相邻差在阈值 0.000 84 m 时,对发生卷渣缺陷判断的召回率高达 0.909,但精确率仅 0.455(F_1=0.606)。

(3)标准差与液位超调幅度在兼顾精确率和召回率方面更均衡, 而 3 秒窗口标准差变化范围与平均相邻差更偏向提升对卷渣发生的敏感度。

参考文献:

[1] 张维维,李晓伟,吕春风. IF 钢冷轧板表面条状缺陷[J]. 钢铁研究学报,2009, 21(7): 59-62.
ZHANG W W, LI X W, LYU C F. Surface sliver defect of cold rolled IF steel sheet[J]. Journal of Iron and Steel Research, 2009, 21(7): 59-62.

[2] 王志政. IF 钢板坯连铸结晶器液面波动原因及控制[J].连铸, 2012 (1): 1-4.
WANG Z Z. Reason and control for slab continuous casting mold level fluctuation of IF steel[J]. Continuous Casting, 2012(1): 1-4.

[3] 罗衍昭,焦会立,庞在刚,李海波,倪有金,赵林. 热轧工艺对超低碳 IF 钢卷渣和面翘皮缺陷的影响[J]. 钢铁,2015, 50(5): 44-48, 80.
LUO Y Z, JIAO H L, PANG Z G, LI H B, NI Y J, ZHAO L. Effect of hot-rolling technology on slag entrapment and surface sliver defects for ultra-low carbon IF steel[J]. Iron & Steel, 2015, 50(5): 44-48, 80.

[4] 罗衍昭,赵长亮,季晨曦,刘延强,周海忱,黄财德,李海波. 汽车板连铸结晶器偏流流场监测及控制现状[J]. 钢铁,2024, 59(11): 21-33, 64.
LUO Y Z, ZHAO C L, JI C X, LIU Y Q, ZHEN H C, HUANG C D, LI H B. Monitoring and control status of bias flow in continuous casting mold for automobile plate[J]. Iron & Steel, 2024, 59 (11): 21-33, 64.

[5] ZHANG K T, LIU J H, CUI H. Effect of flow field on surface slag entrainment and inclusion adsorption in a continuous casting mold [J]. Steel Research International, 2020, 91(2): 1900437.

[6] 陆巧彤,杨荣光,王新华,张炯明,王万军. 板坯连铸结晶器保护渣卷渣及其影响因素的研究[J]. 钢铁,2006(7): 29-32.
LU Q T, YANG R G, WANG X H, ZHANG J M, WANG W J. Water modeling study on factors affecting mold powder entrapment in slab continuous casting[J]. Iron & Steel, 2006(7): 29-32.

[7] SINHA A K, SAHAI Y. Mathematical modeling of inclusion transport and removal in continuous casting tundishes[J]. ISIJ International, 1993, 33(5): 556-566.

[8] 李广焘,龚殿尧,张殿华,梁勋国,陈驰. 数据驱动的热连轧板平直度分类预测[J]. 钢铁,2024, 59(7): 83-93.
LI G T, GONG D Y, ZHANG D H, LIANG X G, CHEN C. Data-driven classification prediction of hot strip flatness[J]. Iron & Steel, 2024, 59(7): 83-93.

[9] 王健豪,方庆,王家辉,罗霄,张华,倪红卫. 基于随机森林预测转炉物料的废钢比计算模型[J]. 钢铁,2024, 59(3): 79-91.
WANG J H, FANG Q, WANG J H, LUO X, ZHANG H, NI H W. Calculation model of steel scrap ratio based on prediction of converter materials by random forest algorithm[J]. Iron & Steel, 2024, 59(3): 79-91.

[10] 包向军,陈凯,郦秀萍,杨筱静,刘骁,陈光. 基于深度学习的转炉煤气发生量预测模型[J]. 钢铁,2024, 59(1): 67-74.
BAO X J, CHEN K, LI X P, YANG X J, LIU X, CHEN G. Prediction model of converter gas production based on deep-learning[J]. Iron & Steel, 2024, 59(1): 67-74.

[11] 王优龙,李维刚,王永强. 基于集成特征选择和 SVR 的热连轧板凸度预测[J]. 钢铁,2024, 59(1): 99-107.
WANG Y L, LI W G, WANG Y Q. Crown prediction of hot strip steel based on integrated feature selection and SVR[J]. Iron & Steel, 2024, 59(1): 99-107.

[12] 梁印,朱航宇,罗林根,刘志,王宝. 基于深度学习钢中非金属夹杂物图像识别[J]. 钢铁,2023, 58(12): 62-70.
LIANG Y, ZHU H Y, LUO L G, LIU Z, WANG B. Image recognition of non-metallic inclusions based on deep learning[J]. Iron & Steel, 2023, 58(12): 62-70.

[13] 刘书超,王国栋,孙杰,彭文,张殿华,袁国. 数据驱动的转炉智能吹炼控制系统的开发与应用[J]. 钢铁,2023, 58(9): 92-103.
LIU S C, WANG G D, SUN J, PENG W, ZHANG D H, YUAN G. Development and application of digital-driven converter intelligent blowing control system[J]. Iron & Steel, 2023, 58(9): 92-103.

[14] 王帅,李强. 联合大数据和神经网络的高炉透气性预报模型[J]. 钢铁,2023, 58(7): 46-53.
WANG S, LI Q. Prediction model of blast furnace permeability by combining big data with neural network[J]. Iron & Steel, 2023, 58 (7): 46-53.

[15] FANG W, HUANG J X, PENG T X, LONG Y, YIN F X. Machine learning-based performance predictions for steels considering manufacturing process parameters: A review[J]. Journal of Iron and Steel Research International, 2024, 31: 1555-1581.

[16] 金友林,包燕平,刘建华,安航航. 不锈钢板坯连铸结晶器内钢/渣界面行为模拟及卷渣分析[J]. 北京科技大学学报,2009, 31(5): 618-624.
JIN Y L, BAO Y P, LIU J H, AN H H. Simulation on steel/slag interfacial behavior and analysis of slag entrapment in a stainless steel slab continuous casting mold[J]. Journal of University of Science and Technology Beijing, 2009, 31(5): 618-624.

[17] 周秋月,朱坦华,张立峰,陈威,袁天祥,刘珍童. 非稳态浇铸对结晶器卷渣定量影响的大涡模拟[J]. 钢铁,2022, 57(4): 68-78.
ZHOU Q Y, ZHU T H, ZHANG L F, CHEN W, YUAN T X, LIU Z T. Large eddy simulation on quantitative influence of unsteady casting on mold slag entrainment[J]. Iron & Steel, 2022, 57(4): 68-78.

[18] 齐新霞,刘国林,包燕平,徐保美. 板坯连铸机结晶器钢液卷渣的水模型研究[J]. 特殊钢,2004, 25(3): 29-31.
QI X X, LIU G L, BAO Y P, XU B M. A Study of water model on slag entrapment of molten steel in mould of slab continuous caster [J]. Special Steel, 2004, 25(3): 29-31.

[19] 周海忱,刘国梁,李海波,邓小旋,季晨曦,罗衍昭. 基于数值模拟的结晶器卷渣在线预测方法[J]. 钢铁,2022, 57(8): 103-110.
ZHOU H C, LIU G L, LI H B, DENG X X, JI C X, LUO Y Z. Online prediction method of slag entrainment in mold based on numerical simulation[J]. Iron & Steel, 2022, 57(8): 103-110.

[20] 冯巍,朱传运,李德强,刘承军,姜茂发. IF 钢板坯连铸结晶器内钢液流动行为的模拟与优化[A]. 2007 中国钢铁年会论文集[C]. 成都:中国金属学会,2007. 1.
FENG W, ZHU C Y, LI D Q, LIU C J, JIANG M F. Simulation and optimization of molten steel flow behavior in continuous casting mold of IF steel slab[A]. Proceedings of 2007 China Steel Annual Conference[C]. Chengdu: The Chinese Society for Metals, 2007. 1.

[21] ZHENG F, CHEN W, ZHANG L F. Effect of mold oscillation on multiphase flow and slag entrainment in a slab continuous casting mold[J]. Metallurgical and Materials Transactions B, 2024, 55: 3784-3797.

[22] CHEN W, ZHANG L F, REN Q, REN Y, YANG W. Large eddy simulation on four-phase flow and slag entrainment in the slab continuous casting mold[J]. Metallurgical and Materials Transactions B, 2022, 53: 1446-1461.

[23] ZHANG Y X, GAO Z G, SUN J C, LIU L L. Machine-learning algorithms for process condition data-based inclusion prediction in continuous-casting process: A case study[J]. Sensors, 2023, 23(15): 6719.

[24] 孙卫平,刘士新. 基于机器学习的连铸生产过程铸坯表面缺陷预测方法[J]. 冶金自动化,2023, 47(6): 57-63.
SUN W P, LIU S X. Machine learning based prediction method of slab surface defects in continuous casting process[J]. Metallurgical Industry Automation, 2023, 47(6): 57-63.

[25] 王复越,任毅,赵坦,崔福祥. 基于决策树算法的钢板探伤预测模型优化[J]. 鞍钢技术,2022(6): 33-38.
WANG F Y, REN Y, ZHAO T, CUI F X. Optimization of prediction model for flaw detection of steel plates based on decision tree algorithm[J]. Angang Technology, 2022(6): 33-38.

[26] LI G, LU C X, GAN M J, WANG Q Q, HE S P. Influence of submerged entry nozzle clogging on the flow field and slag entrainment in the continuous casting mold by the physical model [J]. Metallurgical and Materials Transactions B, 2022, 53: 1436-1445.

[27] BENAVIDEZ E R, BRANDALEZE E, DI GRESIA G, SANTINI L, MARTÍN A. Mould fluxes in the steel continuous casting process[M]//SRINIVASAN M N. Science and Technology of Casting Processes. Rijeka: IntechOpen, 2012: 7.

[28] YIN S, LI X W, GAO H J, KAYNAK O. Data-based techniques focused on modern industry: An overview[J]. IEEE Transactions on industrial electronics, 2014, 62(1): 657-667.

[29] WALL EMERSON R. Mann-Whitney U test and t-test[J]. Journal of Visual Impairment & Blindness, 2023, 117(1): 99-100.

[30] MONTGOMERY D C. Introduction to statistical quality control (eighth edition)[M]. Hoboken: John Wiley & Sons, 2020.

[31] NATRELLA M. NIST/SEMATECH e-handbook of statistical methods[M/OL]. Gaithersburg: National Institute of Standards and Technology, 2020[2024-05-10]. https://www.itl.nist.gov/div898/handbook.

[32] BOX G E P, JENKINS G M, REINSEL G C, LJUNG G M. Time series analysis: Forecasting and control (5th ed)[M]. Hoboken: John Wiley & Sons, 2016.

[33] OGATA K. Modern control engineering (5th ed)[M]. State of New Jersey: Prentice Hall, 2020.

[34] DUAN H Y, WANG X D, YAO M, LIU Y, YU Y. Prediction approach of bulging position and deformation based on Hilbert-Huang transform in slab continuous casting[J]. Metallurgical and Materials Transactions B, 2020, 51: 1656-1667.

[35] CRUZ D M, NORMEY-RICO J E, COSTA-CASTELLÓ R. Repetitive model based predictive controller to reject periodic disturbances[J]. IFAC Proceedings Volumes, 2014, 47(3): 11494-11499.

[36] BISHOP C M. Pattern recognition and machine learning[M]. New York: Springer, 2006.

[37] BREIMAN L. Random forests[J]. Machine Learning, 2001, 45: 5-32.

[38] STROBL C, BOULESTEIX A L, ZEILEIS A, HOTHORN T. Bias in random forest variable importance measures: Illustrations, sources and a solution[J]. BMC Bioinformatics, 2007, 8: 25.

[39] LIPTON Z C, ELKAN C, NARYANASWAMY B. Optimal thresholding of classifiers to maximize F1 measure[M]//CALDERS T, ESPOSITO F, HÜLLERMEIER E, MEO R. Machine Learning and Knowledge Discovery in Databases. ECML PKDD 2014. Lecture Notes in Computer Science. Heidelberg: Springer, 2014: 225-239.

(责任编辑：杨浩雪)